X-ray absorption spectroscopy of copper and iron in sheep digesta

AH Clarkson* & NR Kendall

School of Veterinary Medicine and Science, University of Nottingham, Sutton Bonington Campus, Leicestershire UK. LE12 5RD. Email: andrea.clarkson@notingham.ac.uk. Telephone: +44 (0) 115 951 6447

ABSTRACT

Background: The bioavailable supply of copper to ruminants has long been problematic. Complexities in supply exist due to interactions with other dietary elements in the rumen, most notably with iron or molybdenum in combination with sulphur, which can result in copper binding preventing its absorption. The molybdenum-sulphur-copper interaction has been extensively studied over the years. However, very little is known about the iron-sulphur-copper interaction, especially its mode of action in the gastrointestinal tract.

Methods: In the present work digesta from the rumen and jejunum of sheep fed a high copper, sulphur and iron diet was analysed using X-ray absorption spectroscopy (XAS).

Results: X-ray absorption fine structure (XAFS) and X-ray absorption near edge structure (XANES) indicated that all of the copper and iron had changed in bonding in the rumen and that the oxidation state of the elements had been reduced into a mix of Fe^{2+} & Fe^{3+} and Cu^{+} with some Cu^{0}.

Conclusion: The copper compounds were most likely to be thiol co-ordinated in line with Cu^{+} chemistry. Changes to the copper compounds took place in the jejunum, although thiols were still highly favoured the possible existence of a copper-iron-sulphur complex which also included oxygen and chloride was also observed. This possibly has some resemblance to the crystal structure of bornite.

KEYWORDS

Ruminant, copper, iron antagonism, XAS; supplementation

INTRODUCTION

Iron and copper are both essential trace minerals in ruminant nutrition. However, intakes of over 150 mg Fe/kg can have a significant reduction on copper status in ruminants impacting on health, welfare and production [1–4]. Ruminants frequently consume iron in excess of this from forages (especially autumn herbage), water (principally non-potable sources), and soil (mainly from compacted or acidic soils) [5–8]. All of which can have a marked inhibitory effect on copper uptake and utilisation [9]. This antagonistic effect is unique to ruminants and is absent in monogastric animals and pre-ruminal calves. This indicates the interaction is dependent on a functional rumen [1] and also appears related to the abundance of sulphur in the rumen [10–12]. Despite wide recognition and experimental evidence of the existence of an interaction between these dietary elements [1,9,10,12,13] the mode of interaction between

copper, iron and sulphur has not yet been successfully elucidated. Very little is known about how these elements interact to inhibit copper availability [10].

In theory, within the rumen, iron could react with sulphide forming iron-sulphide complexes. These complexes could then dissociate and exchange with copper in the lower pH of the abomasum forming insoluble copper sulphide; thus decreasing available copper [10,14,15] (Fig. 1). An alternative, more recent theory, is that iron sulphide could react with copper directly, forming a copper-iron-sulphide complex which is non-absorbable [10,16] (Fig. 1).

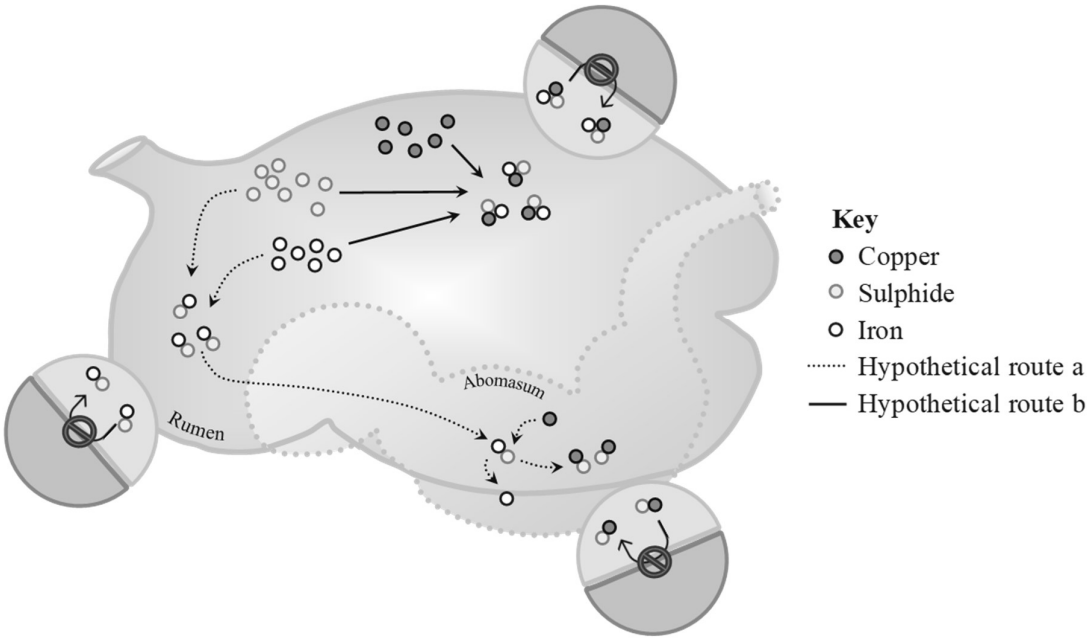

Figure 1: Hypothetical routes for copper antagonism by iron and sulphide. Hypothetical route a (dashed line) shows iron and sulphide combining in the rumen to create insoluble iron sulphide which travels to the abomasum where the lower pH elicits dissociation and exchange for copper creating insoluble copper sulphide. Hypothetical route b (solid line) shows iron, copper and sulphide combining within the rumen to create an insoluble moiety.

The complexity of copper interactions in the rumen have been previously reviewed [10], and are not limited to iron. However, the unique and complex nature of the rumen environment and its microbial population, which cannot be effectively replicated in *in vitro* studies, may be of paramount importance to the mode of action in the iron-sulphur-copper antagonism, and may have prevented the effective elucidation of the mode of action to date. The chemical properties which make copper essential to life, such as its ability to change oxidation state, are also those which make it vulnerable to interaction and binding. The present work aimed to use X-ray absorption spectroscopy (XAS), which has never been previously used on digestive samples of *in vivo* origin to determine the oxidation state of copper and iron in the digesta from two regions of the digestive tract; the rumen and jejunum, from sheep fed a high copper, sulphur and iron diet. The work further aimed to provide information on the local co-ordination bonding of copper and iron in these digestive regions in an attempt progress understanding of the mode of the antagonism.

MATERIALS AND METHODS

Animal experimental

Three 9-10 month old Charollais x lambs (BW ~35 kg) were housed on inedible bedding (HempCore, Aubiose, Buckingham, UK) for a period of 5 days and fed a dried-grass only diet (0.8 kg/day, Graze-on, Northern Crop Driers, York, UK). After this acclimation period, the sheep were additionally fed a daily treatment creating a total elemental inclusion of; 500 mg/kg DM iron ($FeCl_3 \cdot 6H_2O$), 40 mg/kg DM copper ($CuCl_2 \cdot 2H_2O$) and 4 g/kg DM sulphur (Na_2SO_4) from reagent grade sources mixed into 20 g of molasses (NAF, Monmouth, UK) for a period of 48 h prior to slaughter. Animal work was conducted under non-ASPA (AWERB Approval 000166) in line with ARRIVE guidelines. At slaughter, the digestive tract was carefully removed without puncturing. Then sectioned off using two cable ties to secure the junction and cut in between them to section the tract. Rumen and jejunum sections were snap-frozen at the time of culling using an ethanol (>99%, VWR International Ltd, Lutterworth, UK) and solid carbon dioxide (Air Liquide, Stoke-on-Trent, UK) bath (-80 °C). The frozen sections were maintained at -20 °C once completely frozen and cut into smaller sections whilst still frozen using a band saw. The frozen digesta sections from the rumen and jejunum were then cut using a scalpel into blocks ~10 g ww and immediately returned to -20 °C prior to being subject to freeze-drying (Modulyo® M143, Edwards, Leicestershire, UK) until no further weight loss was recorded. Samples were released from vacuum using nitrogen (PRISM, Air products, Surrey, UK) and split into replicates.

Determination of elemental concentration

One replicate was subject to wet acid digestion and ICP-MS to confirm copper and iron concentration. From this replicate, approximately 0.1-0.2 g of freeze-dried digesta was weighed directly into a Teflon microwave digestion tube (HVT50, Anton Paar, St Albans, UK) and incubated for 1 h with 3 ml ≥69.0% HNO_3 (TraceSELECT™, Honeywell Fluka™, Fisher Scientific, Loughborough, UK), 3 ml deionised water (Purite hp 160, Suez, Thame, UK. 17 MΩ cm), and 2 ml 30% H_2O_2 (Fisher Scientific, Loughborough, UK >99%), then digested for 45 minutes (10 min ramp to 140 ˚C, 20 min hold, then 15 min cooling at 55 ˚C) in a Multi-wave 3,000 microwave (Anton Paar, St Albans, UK), alongside blanks and reference material (1577c, Bovine Liver, National Institute of Standards and Technology, USA). Digested samples were transferred and then washed into universal tubes (Sarstedt Ltd., Leicester, UK) with 7 ml of deionised water (Purite hp 160, Suez, Thame, UK. 17 MΩ cm) and inverted to mix, prior to a 500 µl sample taken for ICP-MS (XSeriesII, Thermo Fisher Scientific, Waltham, USA). Samples and calibration standards were diluted (500 µl sample with 9.5 ml diluent) in a diluent containing 0.1% of a non-ionic surfactant (‘Triton X-100’ and ‘antifoam-B’; Sigma Aldrich, Dorset, UK), 2% methanol and 1% HNO_3 (69.0% HNO_3, TraceSELECT™, Honeywell Fluka™, Fisher Scientific, Loughborough, UK), including the internal standards Ir (5 mg/l), Rh (10 mg/l), Ge (50 mg/l) and Sc (50 mg/l). The selection of diluent used for ICP-MS analysis was chosen to supress the fat and foam generated by proteins when plasma samples on the same ICP-MS run. All calibrations were in the range 0-50 mg/l (Claritas-PPT grade CLMS-2 from Certiprep/Fisher Scientific, Loughborough, UK). Results were then calibrated to pre-diluted concentrations and adjusted for background using blank correction.

Digesta preparation for XAS

The second replicate was prepared for XAS analysis by grinding into a homogenous powder using a pestle and mortar and sieving to <120 µm in a nitrogen atmosphere. Ground samples were nitrogen flushed, capped and sealed in the nitrogen atmosphere until analysis. Powdered samples were prepared into aluminium sample holders (Diamond Light Source, Oxfordshire, UK) by careful placement onto a 7 mm square piece of polyamide film (25 µm thickness, DuPont, Stevenage, UK). Samples were compacted with a spatula in the centre to align with the sample holder window at a thickness of 0.5-0.8 mm and covered with a second square of polyamide film secured with silicone adhesive polyamide tape (Kapton®, DuPont, Stevenage, UK) to create a sealed compartment. The back was then screwed on to the sample holder. Standards comprising copper sulphate ($CuSO_4 \cdot 5H_2O$, Acros Organics, New Jersey, USA. 99-102%), iron sulphate ($Fe_2(SO_4)_3 \cdot 9H_2O$, VWR, Leicestershire, UK. >99%), bornite and chalcopyrite (Cu_5FeS_4 & $CuFeS_2$ from crystalline ore. >95% purity, determined by XRD) were prepared into 13 mm diameter pellets using a pelleting press (Atlas 25T, Specac, Kent, UK). Pellets contained 120 mg of reference compound (calculated by formula weight) weighed and mixed into homogeneity with dried cellulose binder in an agate mortar. Standard pellets were analysed in transmission mode alongside a copper or iron foil (I20, Diamond Light Source, Oxfordshire, UK) which were placed in-line with the incident beam with the standards.

XAS Analysis

XAS data for the samples were collected in fluorescence mode at beamline I20-Scanning at the Diamond Light Source (Oxfordshire, UK). Samples were subject to the X-ray beam monochromated by Si (111) crystals. The XAS spectra were collected at the copper (8979 eV) K-edge and iron K-edge (7112 eV). Spectra were recorded in fluorescence mode using the 64-pixel Ge detector (Canberra, Oxfordshire, UK) at 90° to the incident beam. The incident and transmitted X-ray intensities were monitored using ionization chambers. During data collection, samples were maintained at a temperature of -196.15 ˚C using a LN2 cryostat (Oxford instruments, Abingdon, UK) to minimise the effects of radiation damage. For each sample, six to eight 30 min scans for copper K-edge data and six to eight 30 min scans for iron K-edge data were performed due to the dilute nature of the samples. The initial scans were carefully observed for indications of change due to radiation damage. Radiation damage of the sample was observed when a second scan was taken at the same point, therefore the beam position (beam size at sample point HxV = 400 x 300 µm) was adjusted by altering the scan position using the x and y axis between each scan of a distance exceeding 2 mm to ensure each new scan would be performed on undamaged sample. Whilst this design did not calculate how long it would take for the sample to become damaged there was good agreement between the scans and only scans that were identical apart from noise were merged into the final data set mitigating against the effects of damage. The K-range of the XAS spectra was limited to 10 Å due to the presence of a zinc absorption edge at 9659 eV, which distorted the XAS signal beyond this point.

Data analysis

All XAS scans, transmission and fluorescence, were calibrated, aligned, background removed, rebinned and normalised using Athena v 0.9.25 (Ravel and Newville, 2005) generating X-ray absorption near edge structure (XANES) spectra. Where appropriate, scans were merged to reduce the signal to noise ratio at further Å. X-ray absorption fine structure (XAFS) spectra were extracted from μ(E) based on an estimate of the free-atom absorption. Data was extrapolated into K-space where the amplitude and phases were calculated using FEFF[1] to fit χ(k) to a variation of non-linear least-squares curve fitting. Historically, this data type is difficult to evaluate in K-space thus, the data and the fit were transformed through Fourier transform to a radial structure function (R-space) for analysis. XAFS spectra were then peak fitted in R-space using IFFEFIT[1] of Fourier transformed data analysed through Artemis v 0.9.25 (Ravel and Newville, 2005). Goodness of fit was determined where R values were <0.02 and Debye–Waller factors (σ^2) were ~0.02. The likelihood of contributions and similarity to the standards was established through the use of principle component analysis (PCA) and linear combination fitting (LCF). Goodness of fit was determined where R values were <0.02.

RESULTS

XANES of the copper K-edge

Analysis of XANES spectra from XAS data is an interpretive process. Results are extrapolated from the features of the spectra generated in comparison to previous work, crystallographic data and using fingerprinting techniques. The absorption energy (E^0) of the rumen digesta indicates that the average oxidation state of copper in both the rumen and jejunum samples is likely to be between Cu^0 and Cu^+. The E^0 for both rumen and jejunum samples lie very close to the E^0 of metallic copper 8979.3 eV at 8980 and 8981 eV respectively (Fig. 2). This average oxidation is likely to represent some copper in its Cu^+ oxidation state alongside the presence of a notable proportion of Cu^0; elemental or metallic copper. The XANES spectra are identical for the pre-edge and edge regions between the rumen and jejunum samples when plotted in energy (eV) (Fig 2). The only difference is a slightly lower magnitude in the jejunum samples at the edge maxima alongside a slight shoulder at the crest at 8997 eV which is absent in the rumen samples (Fig. 2). However, the spectra differ greatly in the post edge region (8995-9374 eV) especially when the data is plotted in R and K space (Fig. 2). The spectra generated for both digesta samples is more consistent with copper in a three or four co-ordinated geometry, most likely in a tetrahedron. The features of elemental copper at 8981 and 9026 eV are absent and those at 8994 and 9004 eV are largely diminished in the sample spectra. The absence of the edge feature at 8986 eV present on bornite and at 8983 eV on the liver sample suggest that the local co-ordination bonding may be similar but not identical to these compounds. From looking at the spectra it is evident that the copper has changed in bonding from its initial copper compound; divalent (Cu^{2+}) copper chloride as evidenced by the energy shift away from Cu^{2+} and changes in the magnitude and spectra generated (Fig. 2).

[1] IFEFFIT: interactive EXAFS analysis and FEFF fitting. M. Newville, J. Synchrotron Rad. 8, pp 322--324 (2001).

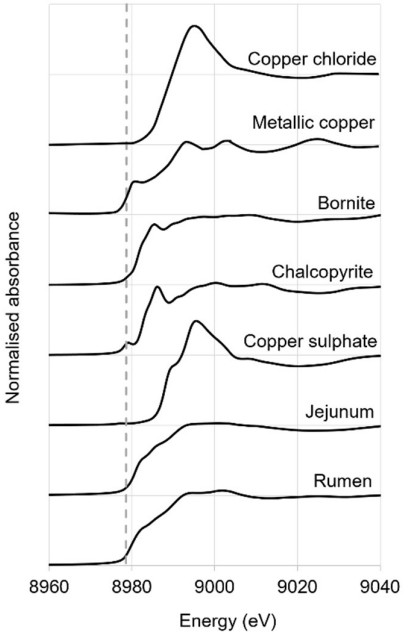

Figure 2. Cu K-edge XANES spectra in energy (eV) for rumen and jejunum digesta samples versus XANES spectra from standards copper$^{(2+)}$ sulphate, chalcopyrite$^{(Cu+)}$, bornite$^{(Cu+)}$ and metallic (elemental) copper$^{(Cu0)}$ and data reported by Klaiphet *et al.*, for copper$^{(2+)}$ chloride.

XAFS peak fitting to the copper K-edge

The XAFS spectra from the rumen and jejunum samples differed greatly (Fig 3), indicating changes in copper bonding as digestion progresses. Analysis of the XAFS data plotted in K-space demonstrated the signal to noise ratio present past 8 Å would negatively impact model fitting results beyond this point. K^2 weighted XAFS data were peak fitted between 1-4.5 Å for the data. Beyond this point the peaks became less distinguishable.

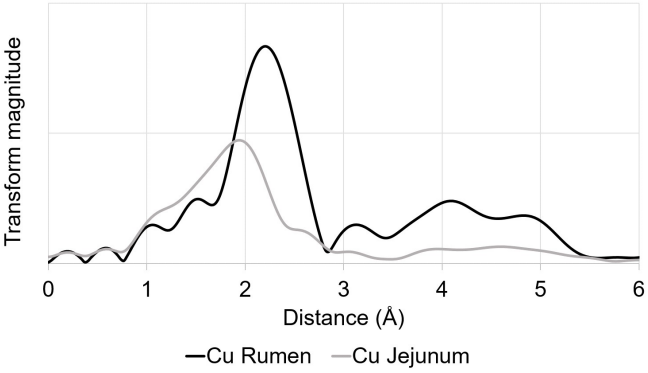

Figure 3. Normalised Fourier transformed copper K-edge data plotted in R-space for rumen and jejunum samples.

The rumen Cu K-edge data initial distance for the first shell was consistent with sulphur, and fitted well with tetrahedral co-ordination, consistent with the XANES spectral observations. All other further paths fitted well with additional copper atoms as single scattering or as a

double forward scattering pathway at 5 Å. The number of fits which were successfully fitted to Cu-Cu were unexpectedly high and showed some similarity to data from the metallic copper standard (Fig 4). The similarity of distance in shells at 2.2, 4.0 and 4.9 Å, although different in magnitude support the XAFS model for Cu-Cu bonds. Additionally, the closeness of E^0 for both rumen and elemental copper suggests that elemental copper may be a contributing compound in the rumen digesta.

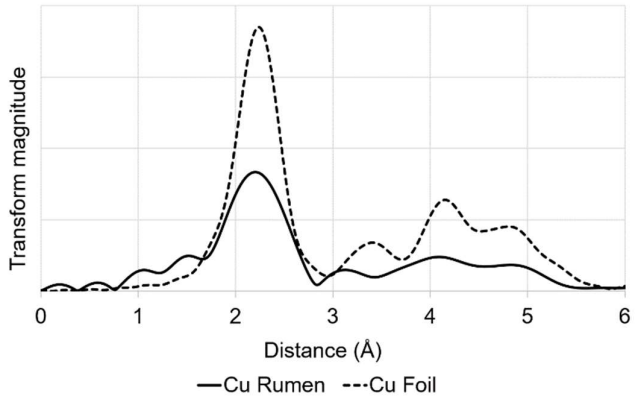

Figure 4. Normalised Fourier transformed copper K-edge data plotted in R-space for rumen sample and metallic (elemental) copper standard.

Table 1. XAFS peak fit n co-ordination number, interatomic distances R(Å) and Debeye-Waller factors σ^2(Å^2) for best fit data for rumen copper K-edge. R-factor indicates goodness of fit (<0.02).

				Co-ordination shell				
Sample	**Path**	**n**	S_0^2	**R(Å)**	**σ^2(Å^2)**	E_0	**Reduced χ^2**	**R-factor**
Rumen	Cu-S	4	0.9	2.096	0.184 (±0.023)	3.64	2735	0.019
	Cu-Cu	6	-	2.553	0.008 (±0.0005)	-	-	-
	Cu-Cu	4	-	3.61	0.013 (±0.004)	-	-	-
	Cu-Cu	6	-	4.421	0.006 (±0.002)	-	-	-
	Cu-Cu-Cu-Cu	8	-	5.105	0.012 (±0.025)	-	-	-

The Cu K-edge data for the first shell of the jejunum sample was fitted with a single scattering oxygen pathway ~1.9 Å followed by three co-ordinated sulphur single scattering pathways at ~2.3 Å, consistent with the XANES observations of tetrahedrally co-ordinated copper. The further shells were less easily defined in this model and were best represented by a single scattering chlorine pathway at ~3 Å (n 2) followed by a double scattering pathway comprising sulphur and iron at ~4 Å (n 4), a further single scattering sulphur pathway at ~4.3 Å (n 3) and lastly a single scattering iron pathway (n 1) at ~4.5 Å (Table 2).

Table 2. XAFS peak fit n co-ordination number, interatomic distances R(Å) and Debeye-Waller factors σ^2(Å^2) for best fit data for jejunum copper K-edge. R-factor indicates goodness of fit (<0.02).

				Co-ordination shell				
Sample	**Path**	**n**	S_0^2	**R(Å)**	**σ^2(Å^2)**	E_0	**Reduced χ^2**	**R-factor**
Jejunum	Cu-O	1	1.05	1.899	0.012 (±0.011)	6.06	1707	0.019
	Cu-S	3	-	2.318	0.013 (±0.005)	-	-	-
	Cu-Cl	2	-	2.914	0.008 (±0.002)	-	-	-
	Cu-S-Fe	4	-	4.102	0.0002 (±0.012)	-	-	-
	Cu-S	3	-	4.371	0.023 (±0.024)	-	-	-
	Cu-Fe	1	-	4.510	0.006 (±0.007)	-	-	-

Principle component analysis (PCA) and linear combination fitting (LCF) models were used to test the similarity of the data to the standards. The rumen data confirmed the XAFS observations that contributions by metallic copper was very likely, and some similarity to bornite was indicated (R 0.007). The jejunum data had similar observations with the most resemblance to bornite and a possible contribution at a lower inclusion for elemental copper (R 0.002).

XANES of the Iron K-edge

The E^0 obtained from the iron K-edge in the rumen and jejunum digesta indicates that the average oxidation state of iron is likely to be a mixture of Fe^{2+} and Fe^{3+} as edges for these samples were at 7124.7 and 7125.2 eV respectively. Close comparison of the E^0 and XANES spectra indicates that the rumen samples contain a higher proportion of iron as Fe^{2+} than those in the jejunum. The spectra for the rumen and jejunum samples are very similar when plotted in energy (eV) (Fig. 5). The E^0 values are very close and the spectral shapes share the same edge features at 7115 eV. The two spectra are differentiated by slight difference in peak magnitude at ~7117 eV and a lower magnitude at the edge maxima in the rumen sample consistent with a higher proportion of Fe^{2+} (Fig. 5). Iron in the digestive samples differs greatly in XANES spectra and E^0 value from the fed compound; iron$^{(3+)}$ chloride, indicating complete speciation from the initial compound. The iron appears to resemble the XANES spectra from iron$^{(3+)}$ sulphate most closely. Both samples and iron$^{(3+)}$ sulphate appear similar in binding energy and spectral shape. Although, the sulphate has a peak of higher magnitude at the edge maxima and the pre-edge features of the samples at ~7115 eV are more pronounced. The spectra share very little commonality with those of chalcopyrite and bornite. There is also some resemblance in XANES spectra to Fe^{2+} sulphide. Which could suggest a mixture of iron$^{(3+)}$ sulphate and iron$^{(2+)}$ sulphide. Although, the spectra differ sufficiently that this cannot be an exact match, it is consistent with the measured oxidation states of the digestive samples and both the pre-edge features and edge maxima occur at similar energies (Fig. 5).

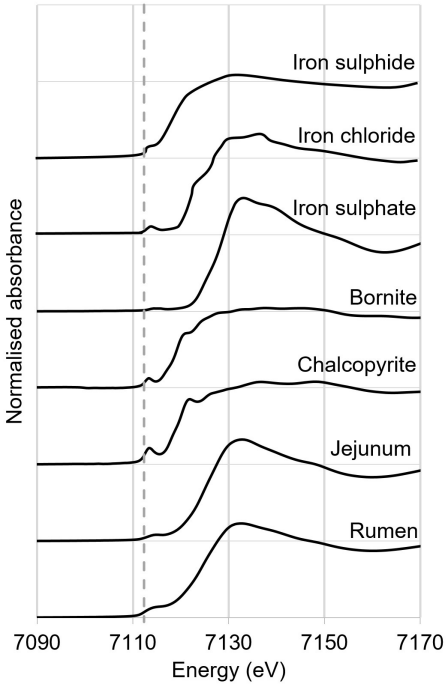

Figure 5: Fe K-edge XANES spectra in energy (eV) for rumen and jejunum digesta samples versus XANES spectra from standards iron$^{(3+)}$ sulphate, chalcopyrite$^{(Fe3+)}$ and bornite$^{(Fe2+)}$ and data reported by He *et al.*, for iron$^{(3+)}$ chloride and data reported by Fittschen *et al.*, for iron$^{(2+)}$ sulphide.

XAFS peak fitting of the iron K-edge

The XAFS spectra for both rumen and jejunum samples at the iron K-edge look superficially different but appear to have similarity with respect to their peak distance (Fig 6). There is similarity in peak distance at 1.5, 2.3, 2.8, 3.4 and 4.4 Å with a similar magnitude at 3.4 Å too. Suggesting that the contributing atoms may be similar but with slightly different bond lengths and co-ordination numbers.

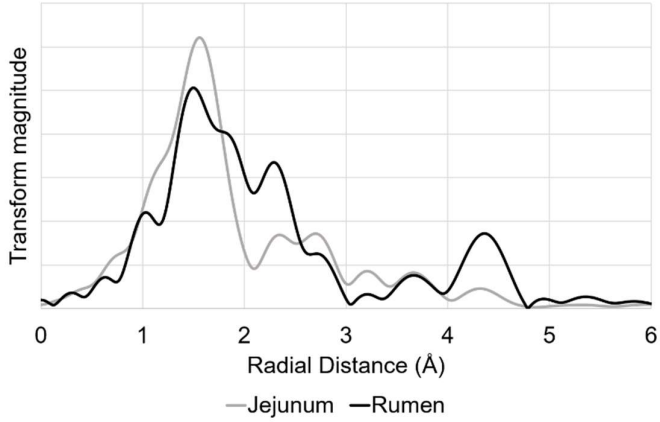

Figure 6. Normalised Fourier transformed iron K-edge data plotted in R-space for rumen and jejunum samples.

The data were both fitted with single scattering oxygen at 1.2 Å (n 3) to fit the initial peak. The XANES spectra for these samples are indicative of tetrahedral, trigonal bi-pyramidal or square pyramidal. Although, increasing the co-ordination to 4 or 5 in these samples reduced the quality of the fit to the initial peak. The next peaks created good fits with single scattering sulphur atoms. The atoms varied in their radial distance and co-ordination number to allow the peak distance and magnitude to be plotted. After 3 Å the sample spectra shares the most similarity, notwithstanding magnitude in some peaks. These peaks were fitted with an oxygen-sulphur obtuse triangle scattering pathway, a single scattering sulphur pathway and an obtuse triangle sulphur-iron scattering pathway respectively, using differing co-ordination to replicate magnitude (Table 3).

Table 3. XAFS peak fit n co-ordination number, interatomic distances R(Å) and Debeye-Waller factors σ^2(Å^2) for best fit data for rumen and jejunum iron K-edge. R-factor indicates goodness of fit (<0.02).

				Co-ordination shell				
Sample	**Path**	**n**	S_0^2	**R(Å)**	**σ^2(Å^2)**	E_0	**Reduced χ^2**	**R-factor**
Rumen	Fe-O	3	0.9	1.997	0.006 (±0.002)	1.86	2423	0.01
	Fe-S	1	-	2.444	0.000 (±0.001)	-	-	-
	Fe-S	2	-	2.636	0.006 (±0.003)	-	-	-
	Fe-O-S	2	-	3.351	0.001 (±0.007)	-	-	-
	Fe-S	8	-	4.043	0.029 (±0.001)	-	-	-
	Fe-S-Fe	8	-	4.776	0.001 (±0.003)	-	-	-
Jejunum	Fe-O	3	1.15	1.997	0.007 (±0.003)	-1.01	743	0.01
	Fe-S	1	-	2.444	0.009 (±0.005)	-	-	-
	Fe-S	4	-	2.636	0.051 (±0.023)	-	-	-
	Fe-O-S	4	-	3.351	0.005 (±0.003)	-	-	-
	Fe-S	8	-	4.043	0.04 (±0.011)	-	-	-
	Fe-S-Fe	4	-	4.776	0.046 (±0.106)	-	-	-

PCA and LCF were conducted on the rumen and jejunum data sets. The results indicated that contributions from iron sulphate were the most likely, with some similarity to bornite, although the model could not fully describe the data set (R 0.019 and R 0.012 respectively).

DISCUSSION

The XAS data provided evidence that copper present in both digestive regions, especially in the rumen, had a high likelihood of being present as Cu^+ with some contribution from Cu^0. The transition from Cu^{2+} into Cu^+ can be explained through the low redox potential (defined as <100 mV, but often negative) of the rumen [19,20]. This environment is sufficient to promote the reduction of Cu^{2+} into Cu^+ using a similar mechanism to the intracellular

environment; which is known to create an environment more conducive to Cu^{+} than Cu^{2+} [21,22] through the maintenance of a cytoplasmic redox potential between -240 and -290 mV [23]. At -350 mV [19], the rumen, although extracellular, creates a strong reducing environment able to promote the spontaneous reduction of dietary Cu^{2+} into Cu^{+} in a similar way. Thermodynamically, the spontaneous reduction of Cu^{2+} into Cu^{+} is supported where the concentration of Cu^{+} is lowered through complexation with the abundant rumen ligands; consequently lowering the ratio of Cu^{+}:Cu^{2+}. Subsequently, Cu^{2+} is reduced to Cu^{+} to re-establish the original ratio valid at the redox potential [24].

Interestingly, the oxidation state of rumen copper was surprisingly close to metallic copper, only 1 eV above the Cu^{0} E^{0}. Photo-reduction can occur in samples where the beam causes radiation damage to the sample reducing the E^{0} [25]. In this experiment the sample position was moved to a distance at least twice the beamline width between each scan to ensure a new area was scanned each time and only identical scans were merged to minimise this effect. Whilst these steps were taken to minimise any beam damage, the scope for photoreduction could not be quantified in the present study. Both the XAFS peak fitting model and XANES spectra demonstrated some resemblance to metallic copper. The results of the PCA and LCF also suggested that there was a component of metallic copper present in the heterogeneous rumen sample despite the limitations of the model preventing an accurate percentage contribution from being obtained.

It is feasible to cycle reversibly between Cu^{0} and Cu^{+} by exposing nanoparticles (<25 nm) to oxidising conditions such as exposure to air, and reducing conditions like those in the rumen environment [26]. Within the rumen there are several strong reducing agents with the potential to elicit an electron exchange to Cu^{0} from Cu^{+} including; Fe^{2+} compounds, sulphite (SO_3^{2-}) containing compounds, sugars which contain a free aldehyde or ketone group (CHO or CO respectively), and even ascorbic acid (vitamin C). Each of which could further reduce copper as Cu^{+} into Cu^{0}. In addition to a low redox potential, unbound Cu^{+} in aqueous solution is able to disproportionate; a reaction where the intermediate ion is able to both oxidise and reduce itself. In this case, Cu^{+} would disproportionate into Cu^{2+} and Cu^{0} following the equation; $2Cu^{+}_{(aq)} \rightleftharpoons Cu^{2+}_{(aq)} + Cu^{0}_{(s)}$ [21]. If the reducing nature of the rumen promotes formation of aqueous Cu^{+} then a proportion of the resulting Cu^{+} could become bound to competing rumen ligands. Since disproportionation can only occur with simple aqueous Cu^{+} complexes, such as Cu^{+} salts in solution, complexation with ligands, other than water, will stabilise the copper in its Cu^{+} state [27]. The remaining proportion of Cu^{+} could potentially disproportionate, producing some Cu^{0} which is stable, and some Cu^{2+} which is instantly reduced into Cu^{+} again by the rumen environment to be subject to further competition. The presence of metallic copper poses a problem for the rumen environment. The microbiota which are present there are fundamentally ill-equipped to handle copper [28–30], and the anti-microbial properties of metallic copper are well documented [31–33], although the mode of action is reliant on direct surface contact with the bacteria and is inhibited in solution [32,33]. Thus, it is possible that a small percentage of the rumen copper could be present as nano-particulate metallic copper.

The evidence gathered in this study indicated that the digestive copper compounds differ notably from the fed copper source which was Cu^{2+} as copper chloride ($CuCl_2 \cdot 2H_2O$). Evidence from the E^{0}, XAFS and XANES spectra all support the notion that this copper

source was subject to dissociation within the rumen and no proportion of copper chloride remained. Previous work has used computer modelling to estimate the likelihood of Cu^{2+} speciation in the bovine rumen from; copper chloride, copper glycine, copper lysine and copper methionine, which found that 60% of copper regardless of initial source was likely to be present as carbonate species, followed by; phosphate (24%), acetate (10%), other volatile acids (4%), ammonia (1%) and aquated copper (0.2%) [34]. The present data agrees that speciation of the copper source takes place, but the present trial did not create a viable XAFS peak fit with Cu^{+} carbonate. The XANES spectra were also very different between the rumen sample data and reference spectra from copper carbonate, copper phosphate, copper acetate, and copper citrate (not shown) indicating that these were not the predominant species of copper present in the rumen. The previous trial used computer modelling in combination with some simulated rumen fluid work to generate their data. It is likely that this model was insufficient to fully replicate the rumen environment and as such may have led to an overestimation of the contribution of salivary complexes (carbonate and phosphate); explaining the absence of these compounds in the *in vivo* data presented here.

The XANES analysis indicated that the rumen compound was likely to be 3 or 4 co-ordinated which was corroborated by the XAFS peak fit which created a good fit with four co-ordinated sulphur atoms in the first shell. The resemblance of XANES spectral shape to bornite, cysteine and Cu^{+} sulphide, all of which comprise Cu^{+} 3 or 4 co-ordinated to sulphur, strongly suggest that the majority of copper in the rumen may be in a Cu^{+} thiol complex. The fit created with tetrahedral sulphur co-ordination in the first shell is inconsistent with metallic copper and the spectra plotted in both energy and R space indicate that at least one other copper containing compound is present. A Cu^{+} thiolate compound is supported by synergistic bonding creating a stable complex [35]. Notably, Cu^{2+} thiolate compounds are known to be unstable in solution and within the rumen could be reduced into Cu^{+}, whereas Cu^{+} sulphur compounds which are either formed or fed are particularly effective at stabilising copper. Using the hard-soft acid-base theory, the soft-soft interaction of Cu^{+} and sulphur will occur more rapidly and form a stronger bond than $Cu^{2+}S$. This principle is also seen in biological thiol complexes. Cu^{2+} complexes with glutathione and cysteine are much less stable than Cu^{+} complexes due to the soft Lewis acid character of Cu^{+} [36]. Glutathione is known to reduce Cu^{2+} to Cu^{+} during complex formation [24], this suggests that in Cu^{+}-thiol complexes Cu^{2+} is first reduced to Cu^{+} in the presence of the thiol and then complexes as a result of the specific complexation of Cu^{+} [24].

Beyond the pre-edge and edge regions the rumen and jejunum copper spectra were very different. The XAFS peak fitting indicated that there were substantial changes in copper speciation between the two regions of the digestive tract. The copper in the jejunum also shared the greatest resemblance in XANES spectra to bornite, cysteine and Cu^{+} sulphide, indicative of a 3 or 4 co-ordinated compound. This compound was successfully XAFS peak fitted with an oxygen-sulphur tetrahedron in its first shell and further shells fitted with chlorine, iron and sulphur. The combination of both iron and sulphur in this fit provide the first insight of a compound containing the elements in the copper-iron-sulphur antagonist pathway. The PCA and LCF showed the greatest similarity to bornite; a copper, iron, sulphur complex known in nature.

Bornite is an insoluble, copper-iron-sulphide with the chemical formula Cu_5FeS_4. Its crystalline shape is orthorhombic at biological temperatures with four sulphur atoms, five copper atoms and one iron atom making up the cubic unit. The first copper atom is tetrahedrally co-ordinated with sulphur with copper in its Cu^+ oxidation state and iron as Fe^{2+} [37,38]. While the jejunum compound shares the tetrahedral co-ordination, in the present model it comprised three sulphur and one oxygen atoms. Due to the partial occupancy of the bornite shell structure it was not possible to create and XAFS peak fit using bornite preventing the similarity of local geometry and co-ordination between these two compounds from being established. However, it is not expected that enough similarity exists between the two compounds for the peak fit to be valid. It appears that only a small similarity exists between these two compounds, but perhaps gives a first insight into a similar structure worthy of further investigation for this antagonist compound.

The XAS data indicated that the effects of the rumen as a reducing environment also affected the oxidation state of iron, albeit to a lesser extent than copper since a proportion of the iron present was still likely to be Fe^{3+} in the heterogeneous sample. There appeared to be a higher proportion of iron as Fe^{2+} in the rumen in comparison to the jejunum. It is possible that in its available Fe^{2+} form, the Divalent Metal Transporter (DMT1) is able to effectively absorb iron in the earlier parts of the small intestine lowering the proportion of Fe^{2+} in the digesta by the time it reaches the jejunum.

The XANES and XAFS spectra were very similar for both digestive regions, differing only in peak magnitude. Suggesting that although some of the compounds may undergo changes the majority of the iron is consistently complexed as it moves through the digestive regions. The spectra and E^0 of the sample data were very different from that of the fed compound, in agreement with the copper data. This suggests that soluble iron compounds can also change their bonding within the rumen environment. A comparison of the XAFS and XANES data suggested that the iron compound was tetrahedrally co-ordinated by three oxygen and one sulphur atom and bore the most resemblance to Fe^{2+} sulphide and Fe^{3+} sulphate, potentially suggesting a mixture involving both species. The abundance of sulphur in the XAFS fit for the further shells could explain the similarity between these spectra. In addition to iron sulphate there was also some resemblance to bornite in the LCF, although the potential contribution by iron sulphate was much greater. Unfortunately, no copper atoms could be successfully fitted into the iron XAFS peak fit. The absence of copper could be explained by a much lesser proportion of iron being involved in the copper-iron-sulphur pathway; perhaps in a similar ratio to that observed in bornite of 5:1 Cu:Fe. Since iron is generally present in a greater concentration than copper in digesta it is possible that the proportion of iron interacting in the copper-sulphur moiety is too small to impact the overall spectra of iron itself. The two main modes of action hypothesized for this pathway suggest that iron may displace copper in the sulphide complex, or, that a copper-iron sulphide complex forms. Both modes of action are still possible based on the evidence from this trial. If a compound similar to copper-iron sulphide is forming it has been indicated to be closer in structure to bornite than chalcopyrite. The elimination of direct sulphide formation cannot be ruled out, the similarity of spectra and number of fits which were enhanced through thiol and sulphur groups show the effects of this abundant ligand in the rumen. The indications from this trial suggest that copper complexation with iron and sulphur may occur beyond the rumen and

may involve a more complex compound involving oxygen and chlorine, most likely as chloride, in addition to copper sulphur and iron.

Acknowledgements

The authors gratefully acknowledge Diamond Light Source for time on Beamline I20 under Proposal SP17053, and the significant contribution and support provided by Dr. I Mikulska, Dr. S Hayama, Dr. S Diaz-Moreno and Dr. F Mosselmans for the experimental and analytical work carried out at Diamond.

This research received no specific grant from any funding agency, commercial or not-for-profit sectors. Although, funding for the wider project was jointly funded by the University of Nottingham, School of Veterinary Science & Medicine and Trouw Nutrition R&D.

Author contributions

AH Clarkson contributed the experimental design in collaboration with the team at Diamond, data collection, analysis and writing of this paper, NR Kendall contributed animal experimental design, supervisory advice and authorship contributions.

Competing interests

The authors declare no conflicts of interest.

REFERENCES

[1] I. Bremner, W.R. Humphries, M. Phillippo, M.J. Walker, P.C. Morrice, Iron induced copper deficiency in calves: Dose-response relationships and interactions with molybdenum and sulphur, Anim. Prod. 45 (1987) 403–414.

[2] A. Prabowo, J.W. Spears, L. Goode, Effects of dietary iron on performance and mineral utilization in lambs fed a forage based diet, J. Anim. Sci. 66 (1988) 2028–2035.

[3] L.A. Mullis, J.W. Spears, R.L. McCraw, Effects of breed (Angus vs Simmental) and copper and zinc source on mineral status of steers fed high dietary iron, J. Anim. Sci. 81 (2003) 318–322.

[4] P.A. Bone, Copper deficiency, molybdenum toxicity and copper toxicity: Where are we now?, Cattle Pract. 18 (2010) 73–75.

[5] W.R. Humphries, M. Phillippo, B.W. Young, I. Bremner, The influence of dietary iron and molybdenum on copper metabolism in calves, Br. J. Nutr. 49 (1983) 77–86. https://doi.org/10.1079/BJN19830013.

[6] S.R. Gooneratne, W.T. Buckley, D.A. Christensen, Review of copper deficiency and metabolism in ruminants, Can. J. Anim. Sci. 69 (1989) 819–845. https://doi.org/10.4141/cjas89-096.

[7] M.R. Coup, A.G. Campbell, The effect of excessive iron intake upon the health and

production of dairy cows, New Zeal. J. Agric. Res. 7 (1964) 624–638. https://doi.org/10.1080/00288233.1964.10416390.

[8] J.W. Spears, Trace mineral bioavailability in ruminants, J. Nutr. 133 (2003) 1506–1509.

[9] A.G. Campbell, M.R. Coup, W.H. Bishop, D.E. Wright, Effect of elevated iron intake on the copper status of grazing cattle, New Zeal. J. Agric. Res. 17 (1974) 393–399. https://doi.org/10.1080/00288233.1974.10421023.

[10] L. Gould, N.R. Kendall, Role of the rumen in copper and thiomolybdate absorption, Nutr. Res. Rev. 24 (2011) 176–182. https://doi.org/10.1017/S0954422411000059.

[11] I. V Rosa, C.B. Ammerman, P.R. Henry, Interrelationships of dietary copper, zinc and iron on performance, Nutr. Rep. Int. 34 (1986) 893–902.

[12] J.F. Standish, C.B. Ammerman, Effect of excess dietary iron as ferrous sulfate and ferric citrate on tissue mineral composition of sheep, J. Anim. Sci. 33 (1971) 481–484.

[13] M. Phillippo, W.R. Humphries, T. Aktinson, G.D. Henderson, P.H. Garthwaite, The effect of dietary molybdenum and iron on copper status, puberty, fertility and oestrous cycles in cattle, J. Agric. Sci. 109 (1987) 321–336. https://doi.org/10.1017/S0021859600080758.

[14] J.D. Allen, J.M. Gawthorne, Involvement of the solid phase of rumen digesta in the interaction between copper, molybdenum and sulphur in sheep, Br. J. Nutr. 58 (1987) 265–276.

[15] N.F. Suttle, P. Abrahams, I. Thornton, The role of a soil × dietary sulphur interaction in the impairment of copper absorption by ingested soil in sheep, J. Agric. Sci. 103 (1984) 81–86. https://doi.org/10.1017/S0021859600043343.

[16] I.K. De Sousa, A.H. Minervino, R.S. Sousa, D.F. Chaves, H.S. Soares, I.O. Barros, C.A. De Araújo, R.A. Barrêto, E.L. Ortolani, Copper deficiency in sheep with high liver iron accumulation, Vet. Med. Int. 2012 (2012) 7–9. https://doi.org/10.1155/2012/207950.

[17] A.L. Ankudinov, B. Ravel, J.J. Rehr, S.D. Conradson, Real space multiple scattering calculation of XANES, Phys. Rev. 58 (1998).

[18] M. Newville, IFEFFIT: interactive EXAFS analysis and FEFF fitting, J. Synchrotron Radiat. 8 (2001) 322–324.

[19] D.N. Kamra, Rumen microbial ecosystem, Curr. Sci. 89 (2005) 124–135. https://doi.org/10.1146/annurev.es.06.110175.000351.

[20] T.G. Nagaraja, Microbiology of the rumen, in: D. Millen, M. De Beni Arregoni, D. Lauritano Pacheco, R (Eds.), Rumenology, Springer US, New York, USA, 2016: pp. 39–61.

[21] D.K. Johnson, M.J. Stevenson, Z.A. Almadidy, S.E. Jenkins, D.E. Wilcox, N.E. Grossoehme, Stabilization of Cu(I) for binding and calorimetric measurements in aqueous solution, Dalt. Trans. 44 (2015) 16494–16505. https://doi.org/10.1039/c5dt02689j.

[22] M.E. Helsel, K.J. Franz, Pharmacological activity of metal binding agents that alter copper bioavailability, Dalt. Trans. 44 (2015) 8760–8770. https://doi.org/10.1039/c5dt00634a.

[23] H.R. López-Mirabal, J.R. Winther, Redox characteristics of the eukaryotic cytosol, Biochim. Biophys. Acta. 1783 (2008) 629–640. https://doi.org/10.1016/j.bbamcr.2007.10.013.

[24] M.F. Leal, C.M. Van Den Berg, Evidence for strong copper(I) complexation by organic ligands in seawater, Aquat. Geochemistry. 4 (1998) 49–75. https://doi.org/10.1023/A:1009653002399.

[25] P.F. Gonçalves, D. De Ligny, O. Lazzari, A. Jean, O.C. Gonzalez, D.R. Neuville, Photoreduction of iron by a synchrotron X-ray beam in low iron content soda-lime silicate glasses, Chem. Geol. 346 (2013) 106–112. https://doi.org/10.1016/j.chemgeo.2012.10.029.

[26] S.D. Pike, E.R. White, A. Regoutz, N. Sammy, D.J. Payne, C.K. Williams, M.S. Shaffer, Reversible redox cycling of well-defined, ultrasmall Cu/Cu2O nanoparticles, ACS Nano. 11 (2017) 2714–2723. https://doi.org/10.1021/acsnano.6b07694.

[27] J.C. Kotz, P.M. Treichel, J. Townsend, D. Treichel, Chemistry and chemical reactivity, 10th ed., Cengage Learning, Boston, USA, 2018.

[28] M. Solioz, H.K. Abicht, M. Mermod, S. Mancini, Response of Gram-positive bacteria to copper stress, JBIC J. Biol. Inorg. Chem. 15 (2010) 3–14. https://doi.org/10.1007/s00775-009-0588-3.

[29] P.G. Ridge, Y. Zhang, V.N. Gladyshev, Comparative genomic analyses of copper transporters and cuproproteomes reveal evolutionary dynamics of copper utilization and its link to oxygen, PLoS One. 3 (2008) e1378. https://doi.org/10.1371/journal.pone.0001378.

[30] L.B. Pontel, F.C. Soncini, Alternative periplasmic copper-resistance mechanisms in Gram negative bacteria, Mol. Microbiol. 73 (2009) 212–225. https://doi.org/10.1111/j.1365-2958.2009.06763.x.

[31] L. Wang, C. Hu, L. Shao, The antimicrobial activity of nanoparticles: Present situation and prospects for the future, Int. J. Nanomedicine. 12 (2017) 1227–1249. https://doi.org/10.2147/IJN.S121956.

[32] S. Mathews, M. Hans, F. Mücklich, M. Solioz, Contact killing of bacteria on copper is suppressed if bacterial-metal contact is prevented and is induced on iron by copper ions, Appl. Environ. Microbiol. 79 (2013) 2605–2611. https://doi.org/10.1128/aem.03608-12.

[33] C. Espírito-Santo, E.W. Lam, C.G. Elowsky, D. Quaranta, D.W. Domaille, C.J. Chang, G. Grass, Bacterial killing by dry metallic copper surfaces, Appl. Environ. Microbiol. 77 (2011) 794–802. https://doi.org/10.1128/aem.01599-10.

[34] J. Essilfie-Dughan, Speciation modelling of Cu(II) in the thiomolybdate contaminated rumen, PhD Thesis. University of Saskatchewan, 2007.

[35] M.A. Rizvi, S.A. Akhoon, S.R. Maqsood, G.M. Peerzada, Synergistic effect of

perchlorate ions and acetonitrile medium explored for extension in copper redoximetry, J. Anal. Chem. 70 (2015) 633–638. https://doi.org/10.1134/S1061934815050093.

[36] A. Le Gall, C.M. Van den Berg, Cathodic stripping voltammetry of glutathione in natural waters, Analyst. 118 (1993) 1411–1415.

[37] J. Zhao, G. Chen, Y. Ngothai, Experimental study of the formation of chalcopyrite and bornite via the sulfidation of hematite: Mineral replacements with a large volume increase, Am. Mineral. 99 (2014) 343–354. https://doi.org/10.2138/am.2014.4628.

[38] S.W. Goh, A.N. Buckley, R.N. Lamb, R.A. Rosenberg, D. Moran, The oxidation states of copper and iron in mineral sulfides, and the oxides formed on initial exposure of chalcopyrite and bornite to air, Geochim. Cosmochim. Acta. 70 (2006) 2210–2228. https://doi.org/10.1016/j.gca.2006.02.007.